Proceedings World Geothermal Congress 2026
Calgary, Canada, June 8 – 11, 2026

Favorable Structural Settings of Geothermal Systems in Active Tectonic Regions: A Global Perspective

James E. Faulds[1*], Nicholas H. Hinz[2], Mary Hannah Giddens[1], Natalie Wigger[3], Isabelle Chambefort[4], Mark Coolbaugh[1]

[1]Great Basin Center for Geothermal Energy, Nevada Bureau of Mines and Geology, University of Nevada, Reno, Nevada, USA 89557; [2]Geologica Geothermal Group, Inc., Reno, Nevada, USA; [3]Missouri Geological Survey, Missouri Department of Natural Resources, Rolla, Missouri, USA; [4]Earth Sciences New Zealand, Wairakei Research Centre, Taupo 3352, New Zealand

*jfaulds@unr.edu

Keywords: Favorable structural setting, hidden geothermal system, rifts, arcs, structural controls

ABSTRACT

Favorable structural settings (FSS) control most relatively high-temperature geothermal systems in active tectonic settings, including the Great Basin region of the Basin and Range province (western USA), Aegean extensional province in western Turkey, western branch of the East African rift, Taupo Volcanic Zone (New Zealand), many volcanic arcs, and elsewhere. They include various fault interaction zones, such as terminations, intersections, step-overs (relay ramps), and accommodation zones in normal fault systems, as well as pull-aparts and displacement transfer zones in transtensional domains. Additional FSS are apparent in magmatic settings, such as dike tips and faults intersecting volcanic centers. However, even in magmatic arcs, FSS along normal fault systems control the majority of geothermal systems, suggesting that extensional strain is a fundamental component of generating the permeability necessary for viable geothermal systems. FSS are typically critically stressed and characterized by structural complexity, closely-spaced faults, and greater proportions of fault breccia vs. fault gouge, which enhance permeability and facilitate fluid flow. FSS commonly comprise ~7 to 10% of continental rifts, with step-overs, fault intersections, and fault terminations most common. Identifying FSS is an important exploration tool that can be employed to locate hidden geothermal systems. Identifying and assessing FSS for hosting hidden systems requires integration of multiple geological and geophysical datasets. In most areas, this process is difficult to automate due to lack of high-resolution lidar, detailed geological maps, and detailed geophysical surveys. Further, many FSS (e.g., fault tips) are characterized by minor faults with minimal surface ruptures, making them difficult to recognize. Nonetheless, FSS can be ranked subjectively based on structural complexity, as well as more quantitatively based on slip rates, slip/dilation tendency, and recency of faulting.

1 INTRODUCTION

Favorable structural settings (FSS) commonly control the locations of higher temperature (>100°C) geothermal systems in active tectonic settings. Curewitz and Karson (1997) provided one of the initial global perspectives of FSS, which included examples from mid-ocean ridges, the Taupo volcanic zone (TVZ) in New Zealand, and the Great Basin region (GBR) of the western USA. More recently, FSS have been described in greater detail from the GBR (Faulds et al., 2006, 2021a; Faulds and Hinz, 2015), TVZ (Rowland and Simmons, 2012), western Turkey (Faulds et al., 2009), East African rift (Hinz et al., 2016, 2018), magmatic arcs (Hinz et al., 2016), and other regions. FSS include various fault interaction zones, such as terminations (i.e., fault tips), step-overs (relay ramps; e.g., Peacock and Sanderson, 1994), and accommodation zones (cf., Faulds and Varga, 1998) in normal fault systems in rifts, pull-aparts and displacement transfer zones (cf., Faulds and Hinz, 2015) whereby strike-slip faults end in arrays of normal faults in transtensional domains, and dike tips and faults intersecting volcanic centers in magmatic settings. Figure 1 shows some of the most common FSS. FSS are typically critically stressed and characterized by structural complexity, closely-spaced faults, and greater proportions of fault breccia vs. fault gouge, which enhance permeability and facilitate fluid flow (e.g., Micklethwaite and Cox, 2005; Faulds and Hinz, 2015; Siler et al., 2018). It is important to stress that geothermal activity along FSS are nearly always associated with Quaternary faults (e.g., Bell and Ramelli, 2007), as permeability along inactive faults appears to be insufficient to facilitate fluid flow from deeper warmer levels to shallow enough depths to support development.

Because FSS control the majority of known geothermal systems in many active tectonic settings, they have become an important proxy for identifying potential locations of hidden or blind geothermal systems, which lack surficial features such as hot springs or steam vents. Hidden systems likely constitute the bulk of geothermal resources in the GBR (Coolbaugh et al., 2006) and probably most geothermal provinces around the world. The hidden nature of many systems stems from geothermal upwellings diffusing into permeable layers at depth (Richards and Blackwell, 2002) and/or impermeable clay caps that are produced by hydrothermal alteration and can trap fluids in the subsurface. The abundance of hidden systems is exemplified in the GBR, where ~39% of the known geothermal systems in Nevada are hidden (Faulds et al., 2021a). Most of these hidden systems were discovered accidentally through drilling of shallow agricultural or mineral exploration holes, and thus many more such systems likely exist. In fact, the largest producing geothermal field in Nevada at McGinness Hills, with three operating power plants generating >150 MWe, is essentially a hidden geothermal system (Nordquist and Delwiche, 2013). Although significant sinter deposits crop out at McGinness Hills, no active hot springs or steam vents have been observed, and the system was originally discovered through mineral exploration wells drilled near the sinter that yielded low concentrations of metals but high subsurface temperatures.

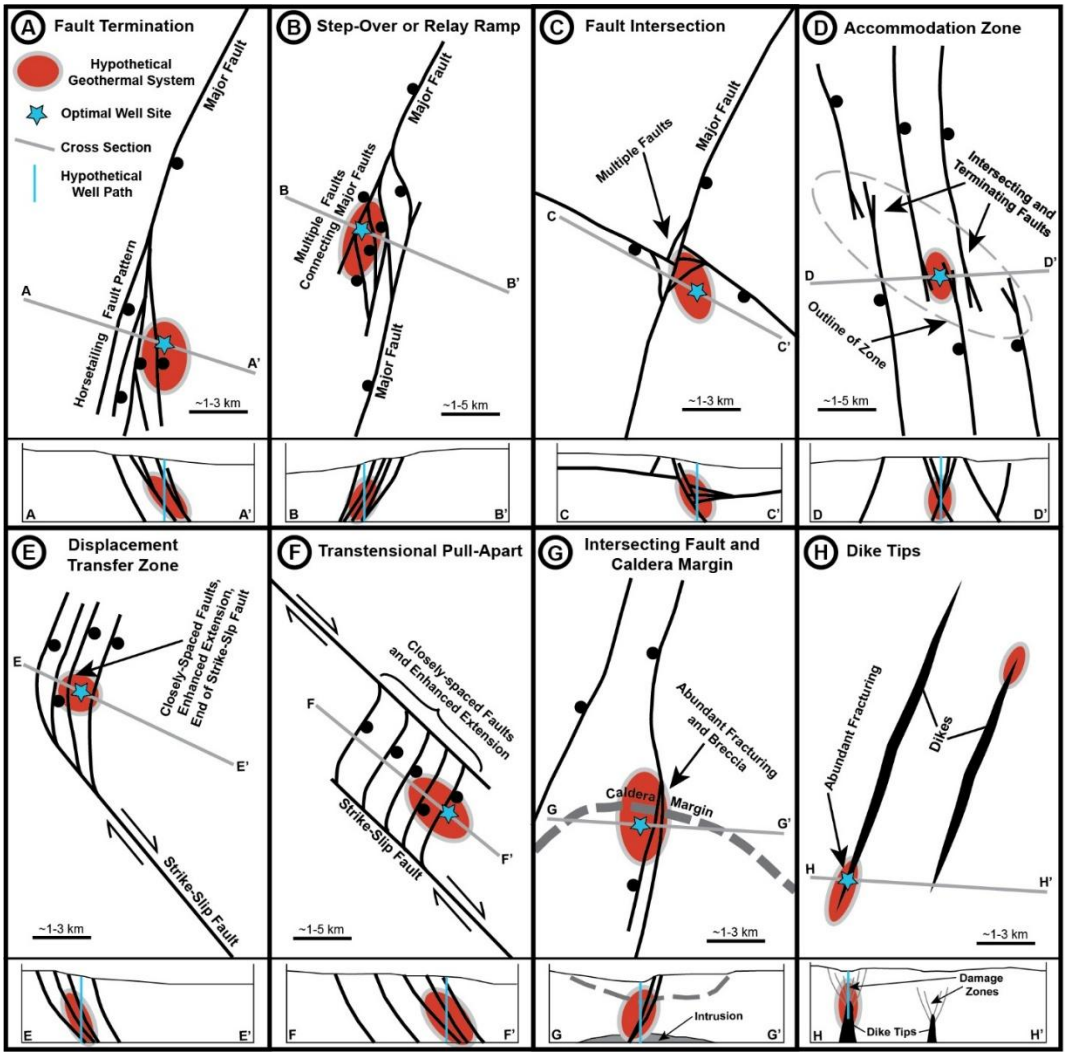


Figure 1. Favorable structural settings for geothermal systems (adapted from Faulds et al., 2021a; Jolie et al., 2021). Most common permeable structures are located in extensional or transtensional settings. Red shaded areas mark approximate locations of hypothetical geothermal upwellings in map view and in cross section. Blue stars and lines illustrate hypothetical optimal well sites and well paths, respectively. a) Fault tip showing horse-tailing pattern of closely spaced faults at the termination of a major normal fault. b) Step-over or breached relay ramp showing abundant minor faults connecting overlapping strands of a major normal fault zone. c) Fault intersection with abundant minor faults proximal to the intersection. d) Accommodation zone (marked by gray ellipse) encompassing systems of oppositely dipping, terminating, overlapping, and intersecting normal faults. e) Displacement transfer zone whereby a major strike-slip fault terminates in an array of normal faults. f) Transtensional pull-apart incorporating multiple closely spaced normal faults connecting a releasing step in a major strike-slip fault. g) Intersecting normal fault

and caldera margin (thick dashed grey line). h) Dike tip or termination, whereby abundant fracturing characterizes the damage zone proximal to the tip of a dike.

Considering the growing body of evidence that FSS play a critical role in controlling geothermal systems, FSS have been used in the past decade as a successful exploration tool to locate hidden geothermal systems (e.g., Faulds et al., 2018; Craig et al., 2021). However, FSS along Quaternary faults are common features in tectonic settings and only some will host a viable geothermal system. Successful exploration therefore relies on integrating other key geophysical and geological datasets that can indicate the location of hidden geothermal systems. These include the distribution of paleo-geothermal deposits that can denote recent geothermal activity (as at McGinness Hills), fluid geochemistry data indicating subsurface temperatures, and various geophysical datasets (e.g., gravity, magnetics, and magnetotelluric data), which can collectively define the subsurface geometry of faults as well as zones of alteration. Workflows and methodologies that allow for integration of multiple datasets into quantitative models, such as play fairway analysis and machine learning techniques, are also important for evaluating and relative ranking of FSS to determine which are most likely to host a hidden system (e.g., Faulds et al., 2021b, c; Craig et al., 2021; Smith et al., 2023). Although significant advancements have been made in utilizing FSS in complex workflows and algorithms, descriptions of the process for identifying FSS have generally been limited to brief accounts. Moreover, since the groundbreaking work of Curewitz and Karson (1997) nearly 30 years ago, global overviews of FSS have been sparse.

In this paper, we therefore describe the process of identifying FSS and then present a global perspective of these features, with examples from both extensional tectonic settings and magmatic arcs in convergent plate boundaries. Extensional tectonic settings include the Great Basin region in the western USA, western Turkey, and East African rift system. Convergent plate boundaries include magmatic arcs and associated subduction zones in the Cascades of western North America, Aleutian Islands in Alaska, and elsewhere. The rapidly extending rifting arc of the TVZ in New Zealand is included in the divergent plate boundary section. These examples capture a large proportion of producing geothermal systems in the world. The global perspective also permits broad comparisons between FSS in a variety of tectonic settings, as well as between magmatic and amagmatic settings.

2 METHODS

Defining FSS is a labor-intensive task that ideally requires access to and analysis of multiple geological and geophysical datasets ranging from regional to local scale. Critical geological datasets include geological maps, Quaternary fault maps, lidar (high-resolution topographic imaging), and digital elevation models. As available, complementary geophysical datasets include gravity, magnetics, and magnetotelluric (MT).

In considering relevant datasets, it is also important to assess the approximate size or scale of FSS, which should reflect the established attributes of known geothermal systems. Volumes are rarely reported in publications. However, the areal extent of resources has been catalogued, with most geothermal systems <20 km^2 and following a lognormal distribution, with the median amagmatic deep circulation system 3 km^2 and the median arc system <4 km^2 (Wilmarth and Stimac, 2020).

Accordingly, the FSS typically range from a scale of hundreds of square meters in area for individual step-overs or fault intersections to tens of square kilometers for larger more complex structures, such as accommodation zones, displacement transfer zones, and pull-aparts. For the larger FSS, initial assessments commonly define relatively broad areas, which can subsequently be broken down into smaller individual FSS (e.g., step-overs or fault intersections) within the larger, more complex structure. The structurally most complex parts of these larger FSS commonly correspond to the locations of geothermal activity (e.g., Dering and Faulds, 2012; Craig et al., 2021). The controlling faults projecting into FSS typically have strike lengths of ~5 to 10 km or greater, although this feature has not been systematically studied.

FSS are best defined by delineating geologically feasible polygons that reflect the surface projection of a geothermal system, as opposed to more rigid rectangles or ellipses. Polygons can more easily encompass the typically irregular boundaries of the geothermal system, while accounting for the surface projection of the vertical dimension. For example, the polygon can be extended toward the down-dip projections of some FSS, such as step-overs, fault terminations, and fault intersections (Figure 1A-C), because such areas would generally correspond to the surface projection of geothermal upwellings at depth.

Digital elevation models accompanied by both regional geological and, where available, Quaternary fault maps (e.g., 1:100,000 and broader scale) can be used to define the larger and/or more conspicuous FSS (e.g., step-overs, accommodation zones, and pull-aparts). For example, the lateral terminations of mountain ranges may roughly define the terminations of normal faults. Topographic steps in the range fronts of mountain ranges/fault

blocks may delineate step-overs or relay ramps. Interbasinal highs commonly correspond to accommodation zones between oppositely dipping Quaternary fault systems. Accommodation zones can also be reflected by a series of low discontinuous ridges associated with intermeshing oppositely dipping normal faults and multiple fault terminations and intersections.

Quaternary fault maps are an important geological dataset, as they provide key insights into the location, geometry, age, and kinematics of active faults, thus defining the locations of FSS. However, such maps are typically of varying quality and commonly do not adequately define key types of FSS (e.g., fault terminations and accommodation zones), where fault displacement may be dying out, and thus associated Quaternary fault scarps are commonly very low relief or possibly absent.

Where available, high-resolution lidar (~1 m resolution) and detailed geological maps (e.g., 1:24,000 to 1:50,000) are generally most useful in defining FSS. Coverage by publicly available high-resolution lidar is quickly increasing in some geothermal provinces (e.g., GBR in the USA), but detailed geological maps are commonly not available. For example, less than 25% of the GBR in the western USA has been mapped at 1:24,000 scale. High-resolution lidar has much greater coverage in the GBR and is therefore essential in defining FSS. Publicly available lidar is generally less common outside the USA. Where publicly available lidar is not available, lidar is commonly acquired by industry and has become a standard dataset to support exploration projects across much of the world.

To sufficiently distinguish the type and location of FSS, it is important to supplement geological data with geophysical data. Gravity is generally the most vital geophysical dataset in defining fault geometries, with isostatic residual and horizontal gradient serving as the most useful. For example, terminating and intersecting gravity gradients can respectively define the tips of major normal faults and fault intersections. Where basins are covered with young sediments, gravity and magnetic data are key to identifying FSS. Even regional gravity datasets have proved useful in defining FSS and should be incorporated where possible. A lesson learned in this regard is the delineation of major fault terminations in the GBR. Initial reviews may interpret fault terminations (i.e., ends of major range-front faults) at the lateral topographic ends of mountain ranges, where conspicuous fault scarps may also die out. However, gravity data commonly show the lateral continuation of these major faults several kilometers into nearby basins, as exemplified by the hidden geothermal system in northern Granite Springs Valley in western Nevada (Faulds et al., 2019). Magnetic and MT data can also be useful in defining subsurface fault geometries and FSS, but both of these datasets are generally more useful in assessing whether an FSS hosts a hidden geothermal system and in defining drill targets. Magnetic lows and low resistivity anomalies may respectively indicate altered rocks and clay caps at depth induced by geothermal activity. Ultimately, delineation of FSS is best accomplished through integration of multiple geological and geophysical datasets utilizing software such as ArcGIS that allows for overlaying multiple data layers.

Notably, the relative importance of datasets can vary depending on local geologic and climatic conditions that can significantly influence the quality and quantity of exposed stratigraphic and structural features while limiting the ability to identify FSS features that are <1 km in length. For example, heavy vegetative cover in places like Indonesia and the Philippines limits the applications of geologic datasets, such as detailed geological maps and in particular, Quaternary fault maps. High-resolution lidar that can see through the vegetative cover is particularly important in such regions. Geophysical datasets can also constrain the structural framework in these regions. Similarly, extensive Quaternary glacial deposits in Alpine regions or high latitudes, as well as Quaternary volcanic deposits and/or basin-fill sediments (especially lacustrine), can hinder the applicability of Quaternary fault maps if the faults have not been particularly active or ruptured since the late Pleistocene. However, high strain rates can mitigate the impacts of relatively wet climates, as demonstrated by the abundance of mapped Quaternary faults in the TVZ of New Zealand (e.g., Villamor and Berryman, 2001; Villamor et al., 2011) and Iceland. In general, relatively arid climates like that in the GBR or western Turkey facilitate more direct application of geological datasets. Although the relative importance of geological and geophysical datasets may vary appreciably according to regional conditions, maps of FSS can generally be produced anywhere so long as local conditions and both the availability and quality of datasets are considered in assessing the quality and uncertainty of the FSS database.

Because FSS may number in the hundreds for individual regions (e.g., Faulds et al., 2021b, c), it is important to develop methods for relative ranking of such features. Although generally subjective, the relative quality and certainty of individual FSS can be estimated. Higher structural complexity is more conducive to geothermal activity, and thus FSS can be ranked, at least qualitatively, based on overall structural complexity, with fault terminations the least complex and accommodation zones, displacement transfer zones, and pull-aparts at the more complex end of the spectrum. Because higher extensional strain rates and higher rates of seismicity

generally correlate positively with geothermal systems (e.g., Faulds et al., 2012; Hart-Wagoner et al., 2024a, b), it also follows that higher slip rates and more recently active Quaternary faults would favor geothermal activity within FSS. Summation of slip and dilation tendency values, based on the orientation of faults with respect to the regional stress field (cf., Morris et al., 1996; Ferrill et al., 1999), are also crucial for evaluating individual FSS. In summary, the quality, certainty, slip rates, recency, and slip and dilation tendency can all be estimated to assess and relatively rank individual FSS within a particular region. Analysis of the most conducive geometries for geothermal activity for individual FSS types can also be employed to assess FSS (e.g., Giddens and Faulds, 2025).

Considering the rapidly increasing coverage of high-resolution lidar in some regions (e.g., GBR of the western USA), an important question is whether the time-consuming process of identifying FSS can be automated employing machine learning and/or image processing techniques. As noted above, lidar and other geological datasets have limitations in many regions due to cover by glacial and lacustrine deposits, and thus FSS identification would ideally involve integration of multiple geological and geophysical datasets. In most areas, this process is difficult to fully automate due to lack of one or more of the key datasets, such as high-resolution lidar, detailed geological maps, and/or gravity data. The lack of pre-competitive geological and geophysical datasets is a major challenge in most geothermal provinces, even those in developed nations (e.g., GBR). Further, some FSS (e.g., fault tips) are characterized by minor faults with minimal surface ruptures, making them difficult to recognize even with high-resolution lidar. Expert-driven oversight is therefore needed in most areas to distinguish actual faults from other features (e.g., paleo-shorelines of Quaternary lakes), define Quaternary faults in bedrock areas, estimate the age of offset surfaces, and ultimately to define FSS.

3 GLOBAL OVERVIEW OF FAVORABLE STRUCTURAL SETTINGS

This section contains an overview of FSS associated with geothermal activity in both divergent and convergent tectonic settings. Divergent settings include regions of continental rifting, transtension, and rifting arcs. The GBR of the Basin and Range province in the western U.S., Aegean extensional province in western Turkey, East African rift, and TVZ in New Zealand are reviewed. Convergent settings include typical magmatic arcs above subduction zones.

3.1 Divergent Tectonic Settings

3.1.1 Great Basin region, western USA

Western North America contains a diffuse plate boundary, characterized by dextral motion between the Pacific and North American plates (e.g., Atwater and Stock, 1998) and west- to northwest-directed extension within the Basin and Range province (e.g., Wernicke, 1992). Much of dextral plate motion (~75%) is taken up by the San Andreas fault system. The other ~25% is distributed across the western GBR in a system of dextral faults known as the Walker Lane in the north and eastern California shear zone in the south (e.g., Faulds and Henry, 2008; Kreemer et al., 2009). A broad zone of active extension that initiated ~30 Ma and has continued into the Quaternary stretches eastward across the GBR from the Sierra Nevada and Walker Lane in eastern California to the Wasatch Front in Utah (Figure 2). Strain rates are generally <1 mm/yr across much of the region but increase to as much as 1 cm/yr within the Walker Lane (Kreemer et al., 2009). The GBR (Figure 2) encompasses most of Nevada, western Utah, eastern California, southern Idaho (south of the Snake River Plain), and southeastern Oregon. It has been one of most tectonically active parts of the Basin and Range province during the Quaternary owing to the diffusion of dextral shear from the northern end of the Walker Lane into regional west-northwest directed extension. This has resulted in relatively high extensional to transtensional strain rates.

With the exception of a few geothermal fields along its margins (e.g., Coso and Long Valley; Figure 2), geothermal systems in the GBR are amagmatic and thus lack a middle to upper crustal magmatic heat source (Blackwell et al., 1999; Faulds et al., 2004, 2006, 2011). Heat in the GBR is provided instead by high geothermal gradients (Blackwell et al., 2011) induced by regional crustal extension and thinning (Blewitt et al., 2005; Faulds et al., 2012). Geothermal systems in this region are generally <225°C. The GBR currently produces ~1 GWe from ~28 geothermal power plants, but estimates suggest far great geothermal potential in the region (e.g., Williams et al., 2009), and hidden geothermal systems may hold the key to unleashing much of this potential. With respect to FSS, the GBR is one of the more heavily analyzed geothermal provinces (e.g., Faulds et al., 2006, 2011, 2021a, b, c; Faulds and Hinz, 2015).

Similar to other extensional settings (e.g., Curewitz and Karson, 1997), geothermal systems in the GBR generally reside in fault interaction zones (Figure 1; Faulds and Hinz, 2015). The INGENIOUS project (INnovative Geothermal Exploration through Novel Investigations of Undiscovered Systems) funded by the U.S. Department of Energy encompasses most of the GBR (Figure 2). A major objective of this project is to generate new

geothermal potential maps of the GBR utilizing ~16 regional datasets. FSS is a key dataset for these maps and includes interpretations of the structural setting for ~400 known geothermal systems, as well as a compilation of more than 1,000 additional FSS of potential hidden systems. Collectively, more than 1,400 FSS were identified and cover ~7.7% of the INGENIOUS study area (Figure 3). Step-overs or relay ramps in normal fault zones are the most common setting, comprising ~40% of the FSS. Such areas are characterized by multiple, commonly overlapping fault strands, increased fracture density, and thus enhanced permeability. Other common FSS include a) fault intersections between two normal faults or between normal faults and transverse oblique-slip faults (26%), b) normal fault terminations (~17%), where horse-tailing generates a myriad of closely-spaced faults; and c) accommodation zones (~7%), where oppositely dipping fault systems overlap in belts of multiple terminating and intersecting faults. Pull-aparts and displacement transfer zones along or adjacent to strike-slip faults account for ~2% and ~1% of the FSS, respectively, but these settings are largely restricted to the transtensional western part of the GBR within or proximal to the Walker Lane and eastern California shear zone. Simple bends in normal faults and the main strands of major normal faults make up very few FSS (~1% and 0.5%, respectively). Magmatic heated, structurally controlled systems (e.g., faults intersecting volcanic centers and dike tips) account for 0.7% of the FSS, whereas hot sedimentary aquifers comprise ~0.1%.

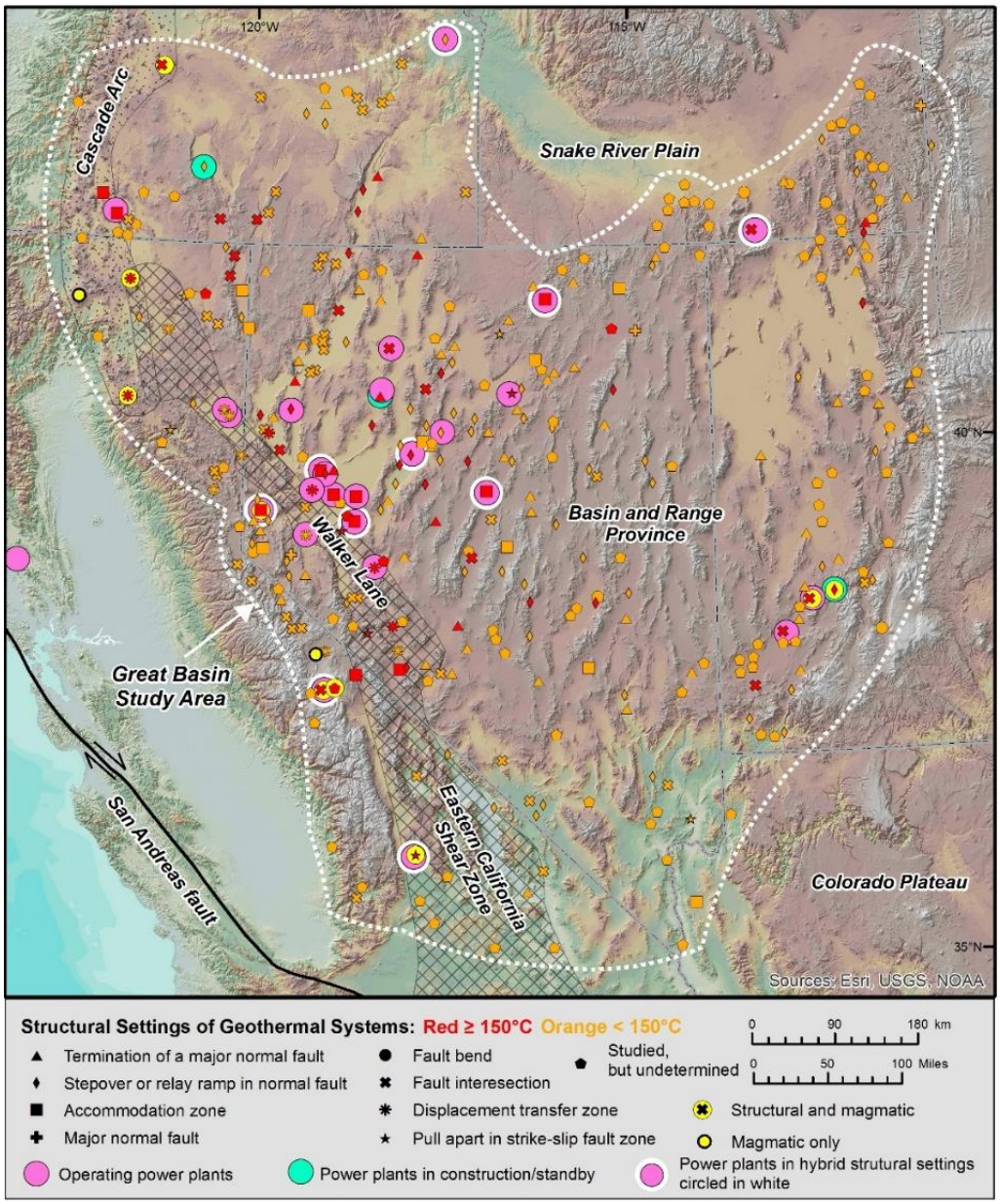


Figure 2. Structural settings of geothermal systems in the Great Basin region (white outline) from Faulds and Hinz (2015). Major types of structural settings are shown on digital elevation model of the Great Basin and adjacent regions. Red symbols – higher-temperature systems (≥150°C); orange symbols – lower-

temperature systems (<150°C); yellow circles represent known or inferred magmatic systems; lavender circles are sites for operating geothermal power plants.

Quaternary faults lie within or near all known, commercial-grade (>120°C) geothermal systems (Bell and Ramelli, 2007). The structural settings for some of the known systems (or ~4% of the FSS) could not be determined. In most cases, undetermined systems reside in the central parts of basins and are only known from warm wells. Regional geophysical datasets (mainly gravity) were assessed to discern the structural controls on these systems. Furthermore, many of these basins are covered by late Pleistocene to Holocene lacustrine sediments, and thus only the most recently active faults can be recognized and related to geothermal activity. Paleo-geothermal deposits (e.g., sinter, silicified sands, and travertine) associated with many of the known systems provide key indicators of relatively recent geothermal activity.

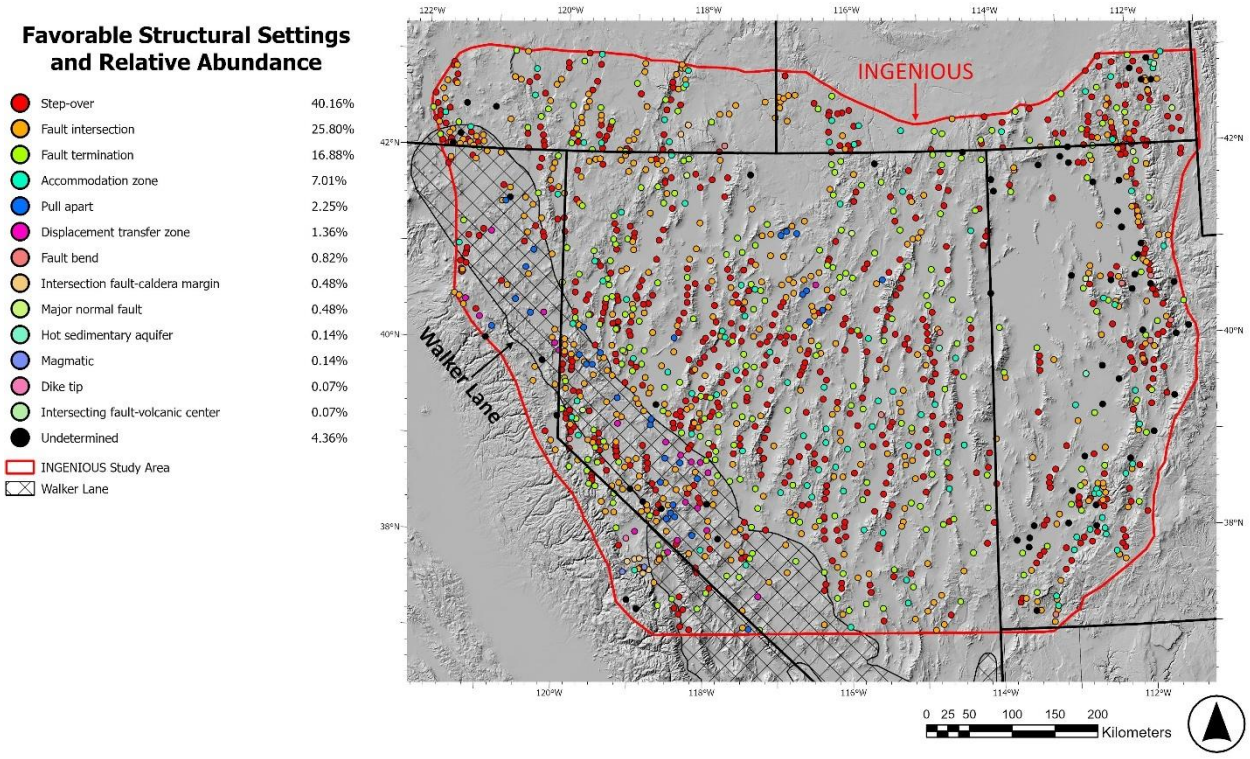


Figure 3. FSS defined for the INGENIOUS study area, which encompasses most of the GBR in the western USA. Relative proportions of the different types of FSS are shown in the legend as percentages of the >1,430 FSS defined in the area. Undetermined FSS represent known geothermal systems for which the structural setting could not be defined.

3.1.2 Western Turkey

Much of western Turkey (Figure 4) has undergone significant ~north-south extension from early Miocene to recent time (Sözbilir, 2001; Seyitoğlu et al., 2002; Işik et al., 2003; Purvis and Robertson, 2004). The first phase of extension occurred in the early to middle Miocene and was related to both gravitational collapse of early Tertiary orogenic highlands and roll-back of the south Aegean subduction zone (Purvis and Robertson, 2004). Major north-south extension has continued into late Miocene to recent time. Major detachment faults remained active into the latest Miocene (Lips et al., 2000). Major steeply dipping normal fault zones that bound major grabens cut Pliocene-Quaternary sediments and some of the detachment faults. In addition, widely spaced (~2 to 5 km) transversely oriented (north-northwest- to north-northeast-striking) oblique-slip faults dissect the region. Late Miocene to recent extension may have been triggered by the westward tectonic escape of the Anatolian block in response to the collision between the Arabian and Eurasian plates (Figure 4; Purvis and Robertson, 2004).

Many of the geothermal systems in this region lie within or along the margins of major ~E-W-trending grabens, which are bounded by major low-angle detachment faults and/or steeply dipping normal fault systems. Recent magmatism in the region has been limited to Quaternary alkaline basalts of the Kula volcanic field (Figure 5; Ercan, 1993; Richardson-Bunbury, 1996; Tokçaer et al., 2005) derived primarily from asthenospheric mantle, with a limited lithospheric mantle contribution and essentially no crustal contamination (Alici et al., 2002). Although proximal to several geothermal fields (Figure 5), including those in the Gediz-Alaşehir graben, the deep

sources for these basalts indicate that related magmas do not provide a direct source of heat for geothermal systems in the region. Thus, western Turkey is characterized by amagmatic geothermal systems related to high geothermal gradients induced by north-south crustal extension and thinning.

Although the structural settings of geothermal systems in western Turkey have not been systematically analyzed, FSS control most known systems (Faulds et al., 2009). Most systems occupy structural discontinuities along ~E-W-striking normal faults, including a) horse-tailing terminations (e.g., Kizildere, Germencik), b) intersections with ~N-striking cross faults (e.g., Salihli, Germencik), c) step-overs in normal fault zones (e.g., Pamukkale, Salihli), d) intersections between multiple normal fault segments (e.g., Simav-Eynal), and e) small pull-aparts in oblique normal-dextral fault zones, especially in the northern part of the region (e.g., Hisaralan west of Simav). In contrast to the GBR in the western USA, fault intersections appear to be the most common FSS hosting known geothermal systems in western Turkey.

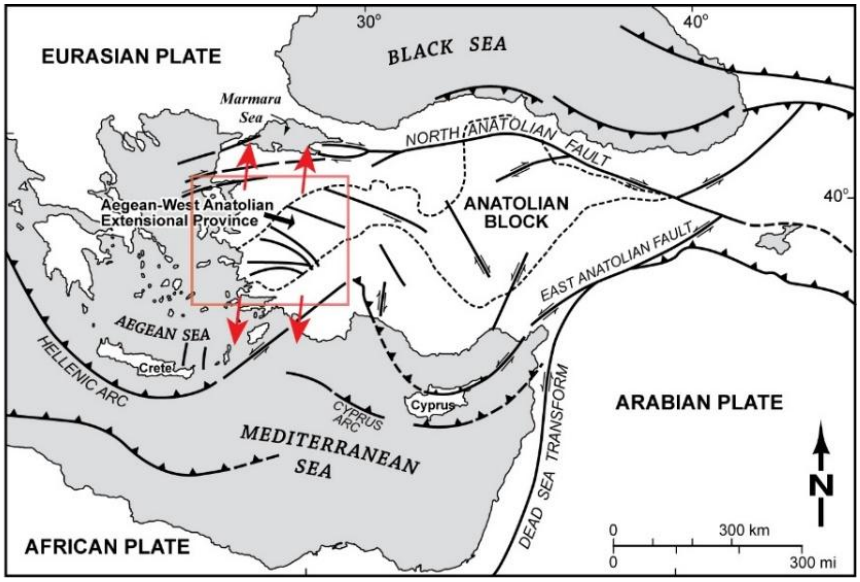


Figure 4. Tectonic setting of Turkey. Slab rollback in the Hellenic arc and westward escape of the Anatolian block, resulting from the collision of the Arabian plate with Eurasia, has induced late Miocene to recent, ~north-south extension (red arrows) in western Turkey. Red box encompasses most of the electricity-producing geothermal systems.

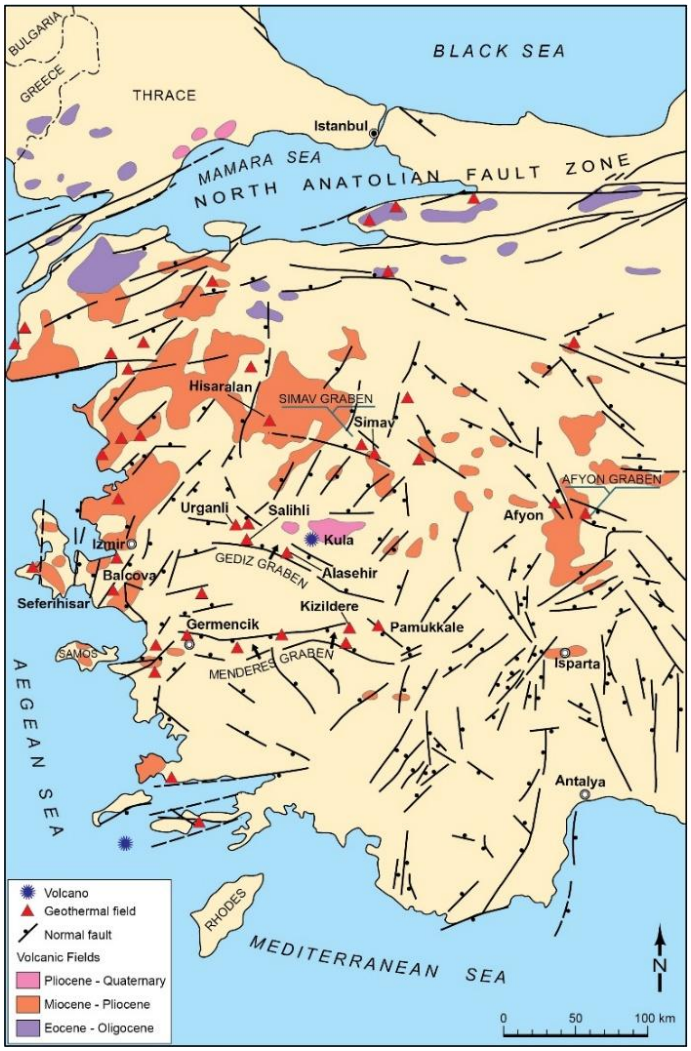


Figure 5. Generalized geologic map of western Turkey showing major fault zones and locations of geothermal systems. Note the lack of Quaternary volcanism. The mantle-derived basalts of the Kula volcanic field are the only Quaternary volcanics in the region.

3.1.3 Western Branch of the East African Rift System (EARS)

The western and eastern branches of the EARS are each associated with different stages of continental rift development (Figure 6). The eastern branch is dominated by magmatic rifting, wherein axial dike intrusion and axial faulting accommodate upper crustal extension (e.g., Morley, 1988; Ebinger and Casey, 2001; Keir et al., 2011). Axial faulting in the active magmatic rift segments has been shown to accommodate >80% of the extension in a given rift segment (Bilham et al., 1999). In contrast to the eastern branch, the western branch of the EARS is dominated by mechanical rifting with extension concentrated along border faults bounding each rift segment. Another contrast between the eastern and western branches is that the volcanic centers in the western branch are mostly fed from deep magmatic sources, with rapid ascent of magma to the surface, imparting minimal heat input to the upper crust.

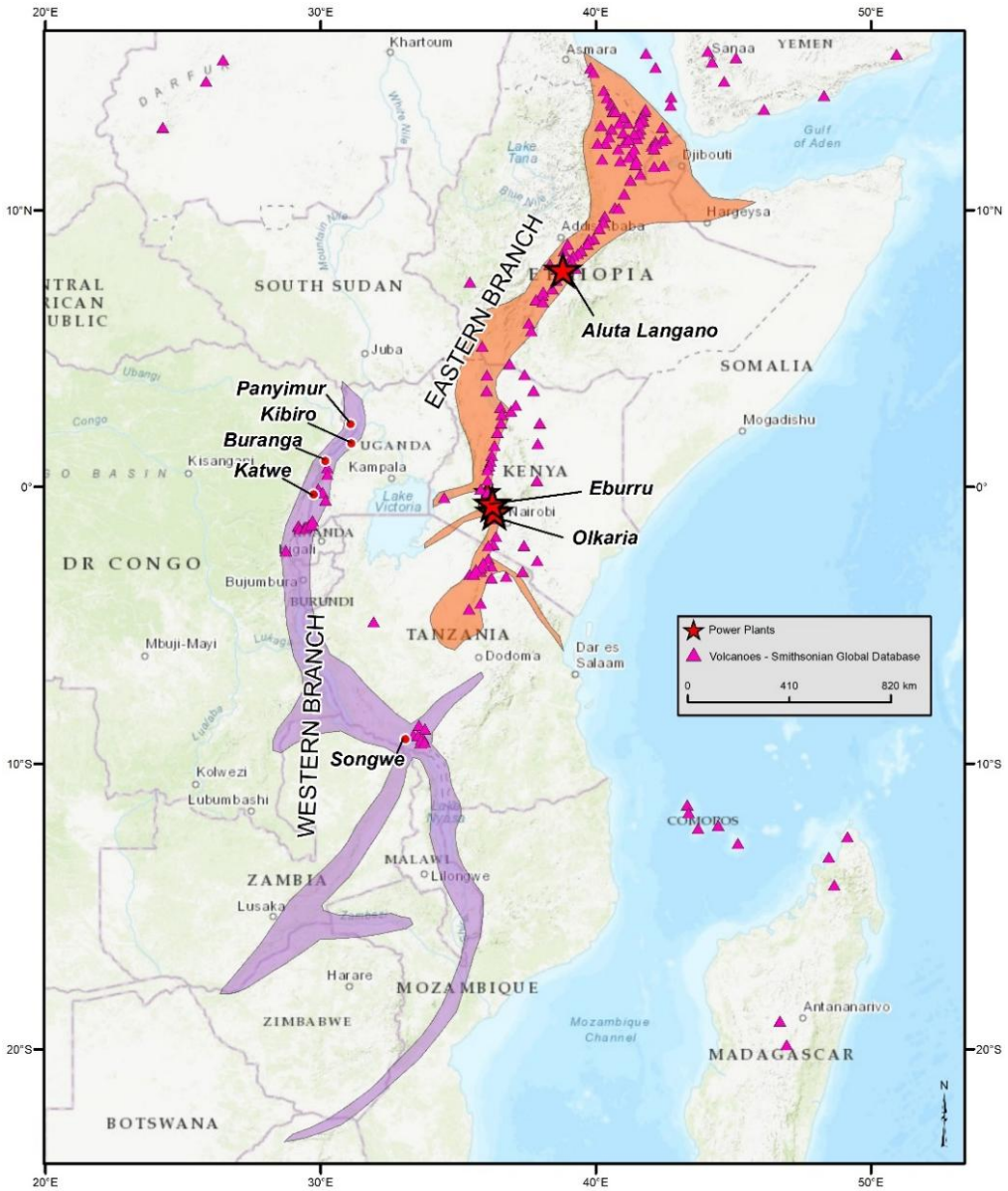


Figure 6. Eastern and western branches of the EARS (adapted from Hinz et al., 2018).

Consistent with the different types of mechanics and magmatism, the eastern and western branches are also associated with different types of geothermal resources. The eastern branch is associated with relatively abundant upper crustal magmatism, and most of the geothermal resources in the eastern branch are high temperature, 230 to 350°C magmatically-heated, volcano-hosted systems (e.g., Olkaria, Kenya and Aluto-Langano, Ethiopia). The eastern branch is also dominated by mafic rift volcanism, and known geothermal systems are most analogous to systems in Iceland. Most of the known geothermal resources in the western rift are <180°C systems heated by deep circulation associated with characteristic structural settings such as fault step-overs or fault intersections (Figures 1 and 6), most analogous to developed resources in the GBR of the Basin and Range province, USA, and in western Turkey. Relatively few of the geothermal resources in the western branch are magmatically heated (e.g., Ngozi, Tanzania), as are < 2% of the known resources in the Basin and Range region (e.g., Long Valley; Faulds and Hinz, 2015) and arguably none of the geothermal resources in western Turkey (Faulds et al., 2009).

Key examples of FSS associated with known geothermal systems in the western branch of the EARS include the Panyimur geothermal area with estimated upflow of ~120°C and the Kibiro geothermal area with estimated upflow of ~125°C in Uganda. Both geothermal systems occupy normal fault step-overs along opposite sides of the Lake Albert basin in Uganda (Hinz et al., 2018). In Tanzania, the Songwe geothermal area with estimated upflow of ~125°C occupies a pull-apart along a strike-slip fault system in the Songwe basin (Hinz et al., 2018). In Zambia, the Bweengwa geothermal area with estimated upflow of ~125 to 150°C occupies a complex step-over zone along a bounding fault on the south side of the Kafue Trough, which is a Permian rift basin that has been

reactivated in the late Cenozoic with renewed extension on the original extensional fault systems (Hinz et al., 2020).

3.1.4 Taupo Volcanic Zone (TVZ), New Zealand

The Taupo Volcanic Zone (TVZ) occupies a dynamic intra-arc rift setting above the Hikurangi subduction zone (Figure 7) and is characterized by relatively high rates of extension, voluminous silicic (in the central TVZ) to intermediate volcanism (in the north and south TVZ), and abundant geothermal activity (e.g., Wilson et al., 1995; Villamor et al., 2011; Holden et al., 2015; Beavan et al., 2016; Wilson and Rowland, 2016). Extensional strain rates generally decrease southward from ~15 mm/yr near the Bay of Plenty to ~7 mm/yr in the Lake Taupo area (Wallace et al., 2004). Extension in the TVZ has been related to rapid clockwise rotation (3-4˚/Myr) of fault blocks in the eastern North Island induced by a complex tectonic setting that includes rollback of the subducting slab and both lateral variations in thickness and oblique convergence between the Pacific and Australian plates (e.g., Wallace et al., 2004). Extension and volcanism began ~2 Ma in the TVZ (Wilson et al., 1995; Milicich et al., 2020). Quaternary volcanic units exceed 2.5 km in thickness in the central part of the rift and typically consist of silicic tuffs and lavas overlying andesitic rocks in some areas (Wilson et al., 1995).

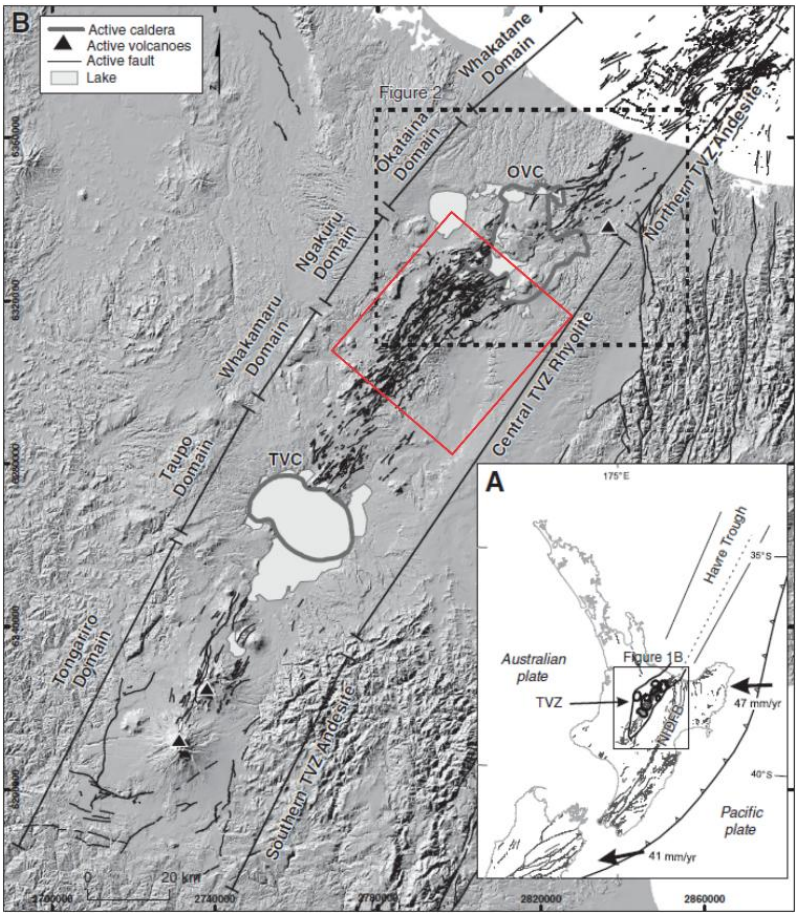


Figure 7. (a) The Taupo Volcanic Zone (TVZ) on the overriding Australian plate of the Hikurangi subduction zone. (b) Area in the Ngakuru graben and Rotorua areas of the central TVZ, outlined by a red rectangle, is shown in Figure 8. This figure is modified from Villamor et al. (2011).

The TVZ is a segmented ~60 km wide rift dominated by closely spaced north-northeast-striking to northeast-striking Quaternary normal fault zones and dike intrusions (e.g., Villamor et al., 2017). Broad west-northwest-trending, transverse accommodation zones bound major rift segments that are marked by discordant axes of extension (Rowland and Sibson, 2004; Rowland and Simmons, 2012). Normal faults generally dip toward the axis of the rift. Faulting is less common in volcanic centers, where dike intrusions probably accommodate significant extension (e.g., Villamor et al., 2011; Rowland and Simmons, 2012). Northwest-southeast extension appears to dominate much of the TVZ (Sibson and Rowland, 2003; Rowland and Simmons, 2012). However, a component of dextral shear has been noted on some north-northeast-striking faults (Acochella, 2003). In addition, parts of the TVZ contain easterly striking (070-085º) normal faults in addition to the north-northeast-striking normal faults (Villamor and Berryman, 2006; Villamor et al., 2017; McNamara et al., 2019).

Structural settings (e.g., especially normal fault step-overs, fault tips, and accommodation zones), similar to those in the GBR, characterize many geothermal fields in the TVZ. For example, the Te Kopia and Orakeikorako geothermal systems occupy a step-over and step-over/fault termination along the Paeroa fault zone, respectively (Rowland and Simmons, 2012). The Waikite geothermal area appears to reside near the northern end of the Paeroa fault, where it breaks into multiple splays and horsetails. The Wai-O-Tapu geothermal field occupies a complex structural setting that includes fault tips and intersections (Curewitz and Karson, 1997), as well intersections between faults and a caldera margin (Rowland and Simmons, 2012). Other robust geothermal systems in the TVZ, such as Wairakei and Rotokawa, are controlled by north-northeast-striking normal faults (e.g., Wallis et al., 2013), but the details of the structural settings are obscured by young volcanic deposits. The youthfulness of the landscape in the TVZ, with late Pleistocene to Holocene volcanic cover in many areas, obscures the structural setting of many geothermal systems. Young volcanic deposits may have completely buried paleo-geothermal features, such as sinter and travertine, thus making it more difficult to explore for recently active and/or hidden geothermal systems.

Geothermal activity in the TVZ is also clearly linked to recent volcanic activity, and volcanic structural features alone can provide sufficient permeability to sustain high-temperature geothermal systems in this high-heat flow environment (Rowland and Simmons, 2012). These structural features include caldera margins, tips of recently intruded dikes, intrusions, and volcanic domes, as well as intersections between any of these features and Quaternary faults. Although many TVZ geothermal fields have surface expressions, additional blind or hidden systems lacking surficial indicators may be present that are not conductive enough to show up in resistivity data (Wilson and Rowland, 2016). Thus, favorable structural settings can be utilized for identifying potential blind geothermal systems in the TVZ. Blind systems may be relatively common in the TVZ, with impermeable clay caps and thick permeable volcanic deposits at depth hindering venting of some systems.

We have therefore prepared preliminary maps of FSS as a proxy for exploration for hidden systems in the TVZ (Wigger et al., 2018; Figure 8). Lidar imagery (GNS Science) and fault databases (Langridge et al., 2016; Seebeck et al., 2022) were used to define the FSS. Owing to the segmented nature of the TVZ and multiple intersections between differently oriented fault sets, FSS are abundant. Discrete fault intersections, step-overs, and terminations are common and amount to nearly 10% of the area. As documented by Rowland and Simmons (2012), accommodation zones are also present, but these tend to be more regional in extent and more difficult to relate to specific exploration targets. It is notable that high fault density in the central TVZ also hinders identification of discrete favorable structural settings. Furthermore, closely spaced inwardly dipping faults in the axial part of the rift define relatively broad zones of intermeshing, oppositely dipping faults or essentially strike-parallel accommodation zones (cf., Faulds and Varga, 1998). Definitive exploration targets are also difficult to define in such areas. Nonetheless, scattered sinter deposits in Quaternary volcanic deposits indicate the likelihood of hidden geothermal systems and buried caldera structures in the TVZ (Chambefort et al., 2021; Bannister et al., 2022) and suggest that delineation of FSS warrants further investigations. A total of 103 FSS were identified. This includes 40 fault terminations (39% of total), 24 domes with and without intersecting faults (23%), 22 fault intersections (21%), 12 large step-overs (12%), four accommodation zones (4%), and one dike termination (1%). Total areal coverage of FSS in the TVZ is ~9.3%. Several areas that may contain hidden geothermal systems were delineated based on the distribution of FSS with respect to known geothermal resources (Figure 8B).

Notably, young volcanic and sedimentary units obscure many structures hosting fluid upwelling. Using faults to identify potential upwelling structures is less applicable to the central TVZ than amagmatic rift settings, such as the GBR or western Turkey, because the TVZ has such a high volume of magmatic output.

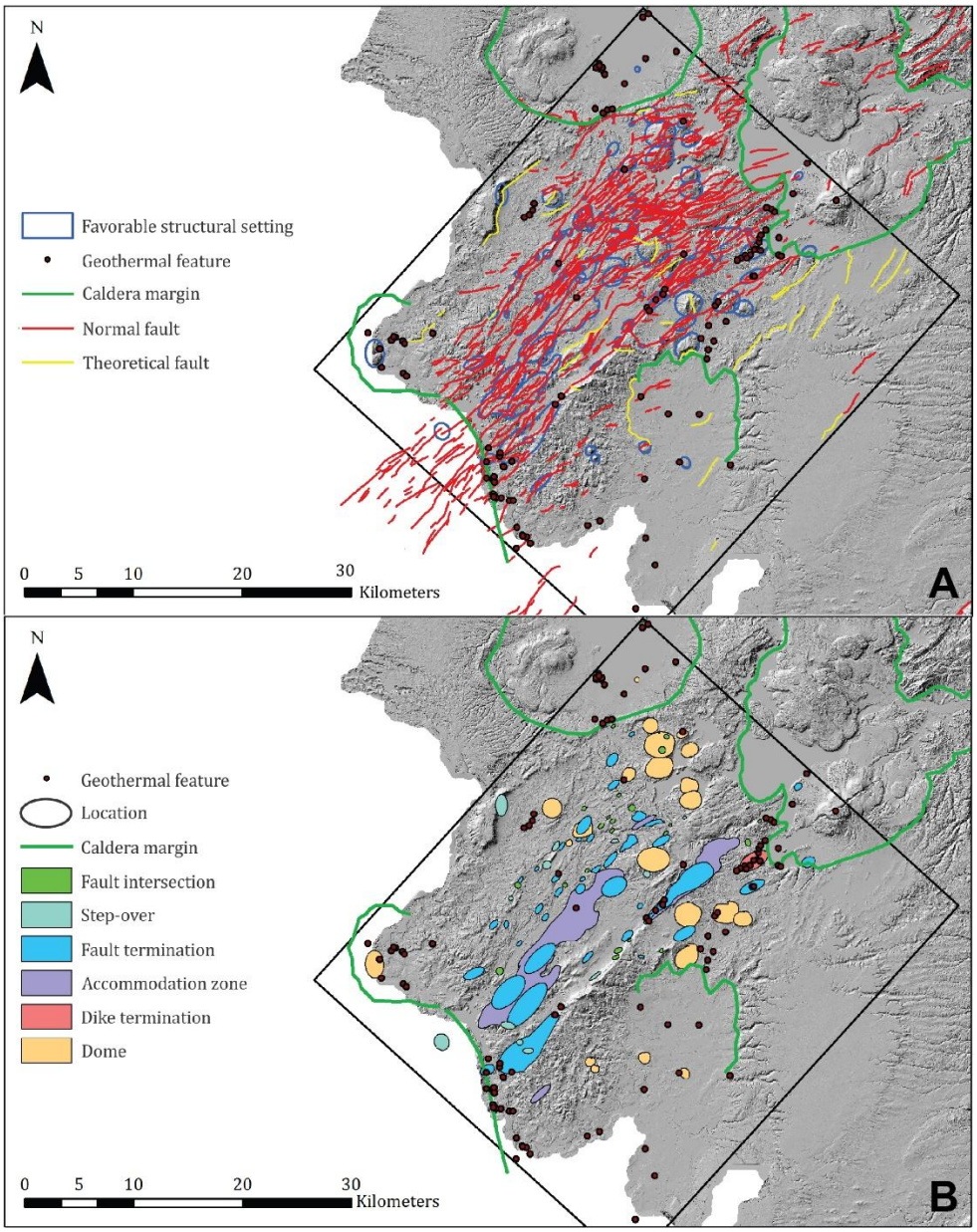


Figure 8. The favorable structural settings of the Rotorua and Ngakuru graben areas in the TVZ of New Zealand. Caldera margins and geothermal feature points are from Leonard et al. (2010). A. Fault data used to define FSS are shown (from Langridge et al., 2016). B. Locations of potential hidden geothermal systems are illustrated.

3.2 Convergent Tectonic Settings – Magmatic Arcs

As of 2015, there were 74 productive geothermal systems in volcanic arcs globally, including actively producing systems, past producing systems, and systems with successful flow tests but not yet developed (Hinz et al., 2016; Shevenell et al., 2015). In arc settings, only a few volcanic centers are associated with multiple geothermal systems. Assuming a near one-to-one ratio of geothermal systems to volcanic centers, these 74 productive volcanic centers constitute ~10% of 732 volcanic centers distributed across more than a dozen major arcs around the world (Figure 9). An inventory of the structural and tectonic settings of these systems was previously completed (Hinz et al., 2016) with comparable methodology to the inventory of systems in the GBR (Faulds and Hinz, 2015). The purpose was to understand if there were favorable intra-arc tectonic patterns that host productive geothermal systems and where sufficient data exist, also catalogue the FSS of each of the 74 productive geothermal systems. These results were originally published by Hinz et al. (2016) and have been summarized here to provide context comparing FSS across all geological settings worldwide.

There are a couple of key patterns in strain accommodation that are consistent in arcs worldwide. One pattern is that the majority of the compressional strain between colliding plates is accommodated in the accretionary wedge. The second is that the majority of the shear strain associated with oblique plate convergence is

commonly accommodated by either intra-arc or arc-marginal deformation, mostly in the form of strike-slip faulting. The intra-arc tectonic setting is highly variable, ranging from extension to transtension, transpression, or compression and may be partly responsible for why some segments of arcs have many large geothermal systems and others do not.

The regional tectonic setting of the 74 geothermal areas includes 11 (15%) extensional, 43 (59%) transtensional, 4 (5%) transpressional, 7 (9%) compressional, and 9 (12%) unknown (Hinz et al., 2016). Importantly, 73% of the systems in extensional or transtensional environments are responsible for 88% of the total known MWe capability in global arc settings. At a local scale, the geothermal systems are associated with a number of structural settings, including 10 (14%) in pull-aparts along strike-slip fault zones, 15 (20%) in displacement transfer zones, where strike-slip faults merge with normal faults, 4 (5%) in normal fault accommodation zones, 7 (9%) in normal-fault step-overs, 22 (30%) in fault intersections, 4 (5%) in other settings, and 12 (16%) in unknown settings. Of these structural settings, the pull-aparts, displacement transfer zones, step-overs, and accommodation zones accounted for 49% of the productive systems and 76% of the total MWe. In contrast, the fault intersections included 30% of the systems but only 16% of the total MWe. One of the primary conclusions is that productive geothermal systems associated with arc systems are utilizing convective heat flow co-located with areas of active, extensional, intra-arc strain.

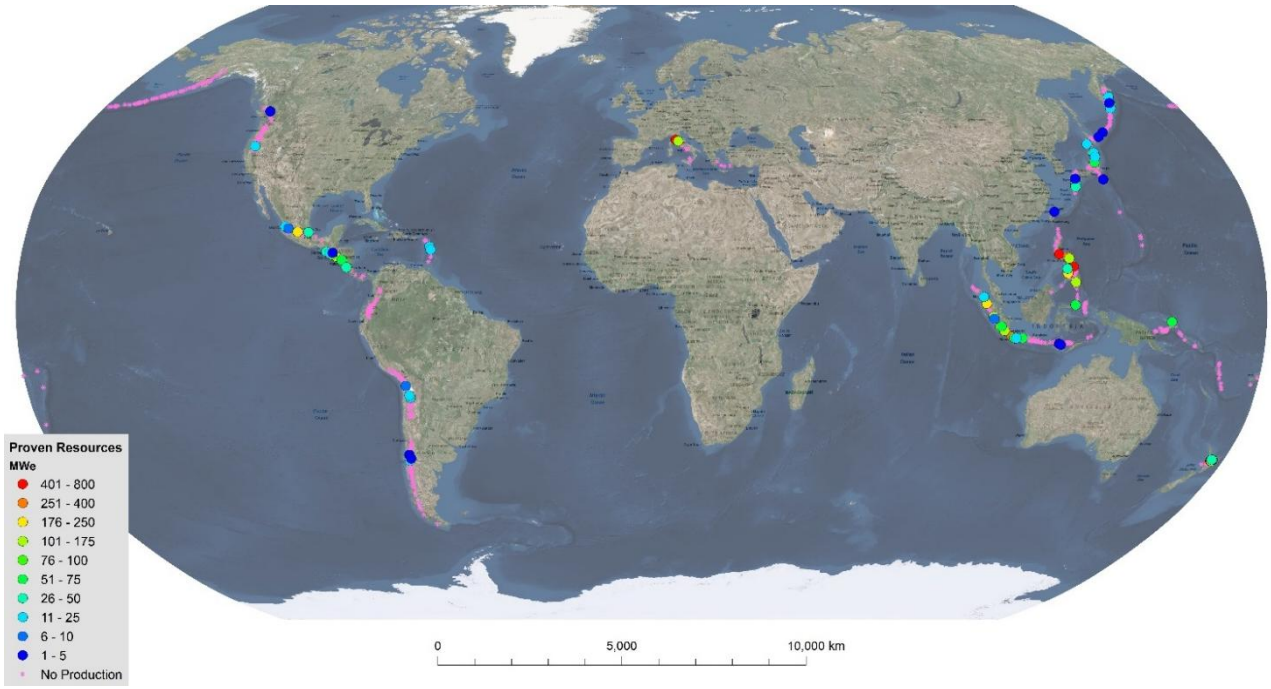


Figure 9. Distribution of globally productive volcanic centers, symbolized by installed MWe category. Background image is from ESRI World Imagery (after Hinz et al., 2016).

4 DISCUSSION

As initially noted by Curewitz and Karson (1997), a relatively small set of FSS (Figure 1) control most of the known geothermal systems in a variety of tectonic settings. This includes extensional and transtensional settings, as well as magmatic arcs in convergent plate boundaries. Typically, extensional strain is most conducive to geothermal activity even in magmatic arcs. FSS include fault tips, fault intersections, step-overs, and accommodation zones in dominantly extensional settings, with displacement transfer zones and pull-aparts prominent in transtensional regions. Additional FSS are apparent in magmatic settings, and these include intersecting faults and volcanic centers and dike tips, but many of the FSS typical of extensional settings are also common in magmatic arcs. This suggests that some level of extensional strain is an important ingredient for geothermal activity in most tectonic settings. This appears to also apply to collisional orogenic belts, as exemplified in the Tibetan Plateau region (e.g., Craig et al., 2026).

Fault interaction zones (i.e., FSS) are more favorable for geothermal activity compared to major normal faults due to multiple factors. Such zones tend to be critically stressed (e.g., Micklethwaite and Cox, 2004; Siler et al., 2018), as stress is generally not relieved by major earthquakes. Faults are therefore less likely to be sealed, allowing for development of relatively long-term hydrothermal systems (Micklethwaite and Cox, 2004). Further, fault gouge is likely to be less prominent and fault breccia more dominant on the relatively minor faults typical

of FSS, as compared to that along major faults. In addition, structural complexity in terms of density of faults and density of fault intersections is probably greater in such zones.

The correlation of the majority of known geothermal systems with a relatively small suite of FSS, as well as the mechanical principles that favor such zones for geothermal activity, suggest that FSS can be used as a tool for identifying potential hidden geothermal systems and ultimately for accelerating geothermal development in a wide array of tectonic settings. However, the process for identifying FSS is dependent on access to geological and geophysical datasets, which are lacking in many regions. The findings in this and other related studies support increasing investment in acquiring precompetitive, publicly available geological and geophysical datasets, such as detailed geological maps (1:24,000 to 1:50,000), Quaternary fault maps, high-resolution lidar, and geophysical datasets (e.g., gravity and magnetics) needed to identify FSS.

It is important to note that more work is needed on FSS to better define their role in controlling geothermal systems, because many FSS have a variety of geometric and kinematic characteristics. For example, step-overs are characterized by several evolutionary stages (e.g., Peacock and Sanderson, 1994), and accommodation zones have multiple possible geometries (e.g., Faulds and Varga, 1998). Certain geometries may be more conducive than others in these FSS (e.g., Giddens and Faulds, 2025), but significant research is needed to establish which characteristics of each FSS are most favorable to geothermal activity. More comprehensive stress modeling is also required to more fully define critically stressed areas and stress perturbations within FSS. Such studies will ultimately reduce the risks in geothermal development of such zones and enhance the probability of discovering many additional hidden geothermal systems.

Acknowledgments

This project was funded by U.S. Department of Energy - Geothermal Technologies Office under award DE-EE0009254 to the University of Nevada, Reno (Nevada Bureau of Mines and Geology). Any use of trade, firm, or product names is for descriptive purposes only and does not imply endorsement by the U.S. Government. We thank Chao Lu for assistance with preparing figures for this study.

REFERENCES

Acocella, V., Spinks, K., Cole, J., Nicol, A., 2003, Oblique back arc rifting of Taupo Volcanic Zone, New Zealand: Tectonics, v. 22. https://doi.org/10.1029/ 2002TC001447.

Alici, P., Temel, A., and Gourgaud, A., 2002, Pb-Nd-Sr isotope and trace element geochemistry of Quaternary extension-related alkaline volcanism: A case study of Kula region (western Anatolia, Turkey): Journal of Volcanology and Geothermal Research, v. 115, p. 487-510.

Atwater, T., and Stock, J., 1998, Pacific-North America plate tectonics of the Neogene southwestern United States - An update. International Geology Reviews, v. 40, p. 375-402.

Bannister, S., Bertrand, E.A., Heimann, S., Bourguignon, S., Asher, C., Shanks, J., and Harvison, A., 2022, Imaging sub-caldera structure with local seismicity, Okataina Volcanic Centre, Taupo Volcanic Zone, using double-difference seismic tomography: Journal of Volcanology and Geothermal Research, v. 431, https://doi.org/10.1016/j.jvolgeores.2022.107653.

Beavan, J., Wallace, L.M., Palmer, N., Denys, P., Ellis, S., Fournier, N., Hreinsdottir, S., Pearson, C., and Denham, M., 2016, New Zealand GPS velocity field: 1995–2013: New Zealand Journal of Geology and Geophysics, v. 59, p. 5-14, DOI: 10.1080/00288306.2015.1112817.

Bell, J.W. and Ramelli, A.R., 2007, Active faults and neotectonics at geothermal sites in the western Basin and Range: Preliminary results: Geothermal Resources Council, v. 31, p. 375-378.

Bignall, G., 2009, Ngatamariki Geothermal Field geoscience overview: GNS Science Consultancy Report, v. 94, p. 41.

Bilham, R., Bendick, R., Larson, K., Braun, J., Tesfaye, S., Mohr, P., and Asfaw, L., 1999, Secular and tidal strain across the Ethiopian rift: Geophysical Research Letters, v. 27, p. 2,789-2,984.

Blackwell D, Wisian K, Benoit D, Gollan B., 1999, Structure of the Dixie Valley Geothermal System, a “Typical” Basin and Range Geothermal system, From Thermal and Gravity Data: Geothermal Resource Council Transactions, v. 23, p. 525-531.

Blackwell, D.D., Richards, M., Frone, Z., and Batir, J., 2011, Temperature-at-depth maps for the conterminous U.S. and geothermal resource estimates: Geothermal Resources Council Transactions, v. 35, p. 1545–1550.

Blewitt, G., Hammond, W.C., and Kreemer, C., 2005, Relating geothermal resources to Great Basin tectonics using GPS: Geothermal Resources Council Transactions, v. 29, p. 331–336.

Chambefort, I., Wilson, C.J.N., and Rowland, J.V., 2021, New (Zealand) perspectives on continental arc geothermal systems – Overview and future prospects: Proceedings of World Geothermal Congress, 11 p.

Coolbaugh, M.F., Raines, G.L., Zehner, R.E., Shevenell, L., and Williams, C.F., 2006, Prediction and discovery of new geothermal resources in the Great Basin: Multiple evidence of a large undiscovered resource base: Geothermal Resources Council Transactions, v. 30, p. 867-873.

Craig, J.W., Faulds, J.E., Hinz, N.H., Earney, T.E., Schermerhorn, W.D., Siler, D.L., Glen, J.M., Peacock, J., Coolbaugh, M.F., and DeOreo, S.B., 2021, Discovery and analysis of a blind geothermal system in southeastern Gabbs Valley, western Nevada, USA: Geothermics, v. 97, p. 102–177.

Craig, J.W., Klemperer, S.L., Crossey, L.J., Karlstrom, K.E., and Winn, C., 2026, Venting the roof of the world: Active faults circulate meteoric fluids through upper-crustal geothermal systems of the Himalaya- Tibet orogen: Geology, v. 54, https://doi .org /10 .1130 /G53940 .1.

Curewitz, D. and Karson, J.A., 1997, Structural settings of hydrothermal outflow: fracture permeability maintained by fault propagation and interaction: Journal of Volcanology and Geothermal Research, v. 79, p. 149-168.

Dering, G. and Faulds, J., 2012, Structural controls of the Tuscarora geothermal field, Elko County, Nevada: Geothermal Resources Council Transactions, v. 36, p. 41-46.

Ebinger, C.M, and Casey, M., 2001, Continental breakup in magmatic provinces: An Ethiopian Example: Geology, v. 29, no. 6, p. 527-530.

Ercan, T., 1993, Interpretation of geochemical, radiometric, and isotopic data on Kula volcanics (Manisa-W. Anatolia): Turkish Geological Bulletin, v. 36, p. 113-129.

Faulds, J.E., and Varga, R., 1998, The role of accommodation zones and transfer zones in the regional segmentation of extended terranes: Geological Society of America Special Paper 323, p. 1-46.

Faulds, J.E., Coolbaugh, M., Blewitt, G., and Henry, C.D., 2004, Why is Nevada in hot water? Structural controls and tectonic model of geothermal systems in the northwestern Great Basin: Geothermal Resources Council Transactions, v. 28, p. 649-654.

Faulds, J.E., Coolbaugh, M.F., Vice, G.S., and Edwards, M.L., 2006, Characterizing structural controls of geothermal fields in the northwestern Great Basin: A progress report: Geothermal Resources Council Transactions, v. 30, p. 69-76.

Faulds, J.E., and Henry, C.D., 2008, Tectonic influences on the spatial and temporal evolution of the Walker Lane: An incipient transform fault along the evolving Pacific – North American plate boundary, *in* Spencer, J.E., and Titley, S.R., eds., Circum-Pacific Tectonics, Geologic Evolution, and Ore Deposits: Tucson, Arizona Geological Society, Digest 22, p. 437-470.

Faulds, J.E., Bouchot, V., Moeck, I., and Oğuz, K., 2009, Structural controls of geothermal systems in western Turkey: A preliminary report: Geothermal Resources Council Transactions, v. 33, p. 375-383.

Faulds, J.E., Coolbaugh, M.F., Hinz, N.H., Cashman, P.H., and Kratt, C., Dering, G., Edwards, J., Mayhew, B., and McLachlan, H., 2011, Assessment of favorable structural settings of geothermal systems in the Great Basin, western USA: Geothermal Resources Council Transactions, v. 35, p. 777-784.

Faulds, J.E., Hinz, N.H., Kreemer, C., and Coolbaugh, M.F., 2012, Regional patterns of geothermal activity in the Great Basin region, western USA: Correlation with strain rates: Geothermal Resources Council Transactions, v. 36, p. 897-902.

Faulds, J.E., and Hinz, N.H., 2015, Favorable tectonic and structural settings of geothermal settings in the Great Basin Region, western USA: Proxies for discovering blind geothermal systems: Proceedings, World Geothermal Congress 2015, Melbourne, Australia, 6 p.

Faulds, J.E., Craig, J.W., Coolbaugh, M.F., Hinz, N.H., Glen, J.M., DeOreo, S., 2018, Searching for blind geothermal systems utilizing play fairway analysis, western Nevada: Geothermal Resources Council Bulletin, v. 47, p. 34-42.

Faulds, J.E., Hinz, N.H., Coolbaugh, M.F., Ramelli, A., Glen, J.M, Ayling, B.A., Wannamaker, P.E., DeOreo, S.B., Siler, D.L., and Craig, J.W., 2019, Vectoring into potential blind geothermal systems in the Granite Springs

Valley area, western Nevada: Application of the play fairway analysis at multiple scales: Proceedings 44th Workshop on Geothermal Reservoir Engineering, Stanford University, Stanford, California, SGPTR-214, p. 74-84.

Faulds, J.E., Coolbaugh, M.F., and Hinz, N.H., 2021a, Inventory of structural settings for active geothermal systems and late Miocene (~8 ma) to Quaternary epithermal mineral deposits in the Basin and Range province of Nevada: Nevada Bureau of Mines and Geology Report 58, 28 p.

Faulds, J.E., Hinz, N.H., Coolbaugh, M., Ayling, B., Glen, J., Craig, J.W., McConville, E., Siler, D., Queen, J., Witter, J. and Hardwick, C., 2021b, Discovering blind geothermal systems in the Great Basin region: An integrated geologic and geophysical approach for establishing geothermal play fairways: All phases: Department of Energy, Geothermal Technologies Office, Final Technical Report on Award DE-EE0006731, 74 p.

Faulds, J.E., Hinz, N.H., Coolbaugh, M.F., Craig, J.W., Glen, J.M., Ayling, B.F., Sadowski, A.J., Siler, D.L, and DeOreo, S., 2021c, The Nevada geothermal play fairway project: Exploring for blind geothermal systems through integrated geological, geochemical, and geophysical analyses: Proceedings World Geothermal Congress 2021, Reykjavik, Iceland, 12 p.

Ferrill, D.A., Winterle, J., Wittmeyer, G., Sims, D., Colton, S., Armstrong, A., Horowitz, A.S., Meyers, W.B., and Simons, F.F., 1999, Stressed rock strains groundwater at Yucca Mountain, Nevada: GSA Today, v. 9, p. 2–9.

Giddens, M.H., and Faulds, J.E., 2025, Analysis of step-overs (or relay ramps) in normal fault systems in the Great Basin region, western USA: Implications for geothermal exploration and development: Proceedings, 50th Workshop on Geothermal Reservoir Engineering, Stanford University, SGP-TR-229, 9 p.

Hart-Wagoner, N., Coolbaugh, M., Faulds, J.E., Mlawsky, E., Lindsey, C., & Trainor-Guitton, W., 2024a, Preliminary regional play fairway workflow for the Great Basin region, USA: Proceedings of the 49th Workshop on Geothermal Reservoir Engineering, Stanford University, Stanford, California, SGP-TR-227.

Hart-Wagoner, N.R., Lindsey, C., Trainor-Guitton, W., Coolbaugh, M., and Faulds, J.E., 2024b, Exploring geothermal potential of Great Basin sub-regions: Geothermal Resources Council Transactions, v. 48, 20 p.

Hinz, N.H., Coolbaugh, M., Shevenell, L., Melosh, G., Cumming, W., and Stelling, P., 2016, Structural–tectonic settings for globally productive subduction arc volcanic centers: Proceedings, 41st Workshop on Geothermal Reservoir Engineering, Stanford University, Stanford, CA, Feb. 22-24, 8 p.

Hinz, N.H., Cumming, B., and Sussman, D., 2018, Exploration of fault-related deep-circulation geothermal resources in the western branch of the East African Rift System: Examples from Uganda and Tanzania: Proceedings, 7th African Rift Geothermal Conference, Kigali, Rwanda, 31st October – 2nd November, 2018, 16 p.

Hinz, N.H., Vivian-Neal, P., Haizlip, J., Matson, G., Cumming, W., Harrison, P., and Campbell, S., 2020, Zambia: Conceptual Model and Drilling Update of the Deep Circulation Bweengwa River Geothermal Prospect: World Geothermal Congress, 16 p.

Holden, L., Wallace, L., Beavan, J., Fournier, N., Cas, R., Ailleres, L., and Silcock, D., 2015, Contemporary ground deformation in the Taupo Rift and Okataina Volcanic Centre from 1998 to 2011, measured using GPS: Geophysical Journal International, v. 202, p. 2082–2105.

Işik, V., Seyitoğlu, G., and Çemen, I., 2003, Ductile-brittle transition along the Aleşehir detachment fault and its structural relationship with the Simav detachment fault, Menderes massif, western Turkey: Tectonophysics, v. 374, p. 1-18.

Jolie, E., Scott, S., Faulds, J., Chambefort, I., Axelsson, G., Gutiérrez-Negrín, L., Regenspurg, S., Ziegler, M., Ayling, B., Richter, A., and Zemedkum, M.T., 2021, Geological controls on geothermal resources for power generation: Nature Reviews Earth and Environment, v. 2, p. 324-339; doi.org/10.1038/s43017-021-00154-y.

Keir, D., Belachew, M., Ebinger, C.J., Kendall, J.M., Hammond, J.O.S., Stuart, G.W., Ayele, A., and Rowland, J.V., 2011, Mapping the evolving strain field during continental breakup from crustal anisotropy in the Afar Depression: Nature Communications, 7 p. DOI: 10.1038/ncomms1287.

Kreemer, C., Blewitt, G., and, Hammond, W.C., 2009, Geodetic constraints on contemporary deformation in the northern Walker Lane: 2. Velocity and strain rate tensor analysis, in Late Cenozoic Structure and Evolution of the Great Basin-Sierra Nevada Transition, eds. J.S. Oldow, and P.H. Cashman, Geological Society of America Special Volume 447, p. 17-31.

Langridge, R.M., Ries, W.F., Litchfield, N.J., Villamor, P., Van Dissen, R.J., Rattenbury, M.S., Barrell, D.J.A., Heron, D.W., Haubrock, S., Townsend, D.B., Lee, J.A., Cox, S., Berryman, K.R., Nicol, A., Stirling, M., 2016, The New Zealand active faults database: NZAFD250: New Zealand Journal of Geology and Geophysics, v. 59 p. 1.

Leonard, G. S., Begg, J. G., & Wilson, C. J. N., 2010, Geology of the Rotorua area: Institute of Geological and Nuclear Sciences, 1:250,000 geological map 5.

Lips, A.I., Cassard, D., Sozbilir, H., Yilmaz, H., and Wijbrans, J.R., 2000, Multistage exhumation of the Menderes massif, western Anatolia (Turkey): International Journal of Earth Sciences, v. 89, p. 781-792.

McNamara, D.D., Milicich, S.D., Massiot, C., Villamor, P., McLean, K., Sépulveda, F., and Ries, W.F., 2019, Tectonic controls on Taupo Volcanic Zone geothermal expression: Insights from Te Mihi, Wairakei Geothermal Field: Tectonics, v. 38, p. 3011–3033. https://doi.org/10.1029/2018TC005296.

Micklethwaite, S., and Cox, S.F., 2004, Fault-segment rupture, aftershock-zone fluid flow, and mineralization: Geology, v. 32, p. 813–816, doi:10.1130/G20559.1.

Milicich, S. D., Chambefort, I., Wilson, C.J.N., Alcaraz, T.R., Ireland, C., Bardsley, M.P., and Simpson, M.P., 2020, A zircon U-Pb geochronology for the Rotokawa geothermal system, New Zealand, with implications for Taupō Volcanic Zone evolution: Journal of Volcanology and Geothermal Research, v. 389; https://doi.org/10.1016/j.jvolgeores.2019.106729.

Morley, C., 1988, Variable extension in Lake Tanganyika: Tectonics, v. 7, p. 785-801.

Morris, A., Ferrill, D.A., and Henderson, D.B., 1996, Slip-tendency analysis and fault reactivation: Geology, v. 24, p. 275–278.

Nordquist, J., and Delwiche, B., 2013, The McGinness Hills geothermal project: Geothermal Resources Council Transactions, v. 37, p. 58–64.

Peacock, D.C.P., and Sanderson, D.J., 1994, Geometry and development of relay ramps in normal fault systems: American Associations of Petroleum Geologists Bulletin, v. 78, p. 147-165, doi:10.1306/BDFF9046-1718-11D7-8645000102C1865D.

Purvis, M., and Robertson, A., 2004, A pulsed extension model for the Neogene recent E-W-trending Aleşehir graben and the NE-SW-trending Selendi and Gordes basins, western Turkey: Tectonophysics, v. 391, p. 171-201.

Richards, M., and Blackwell, D., 2002, A difficult search: Why Basin and Range systems are hard to find: Geothermal Resources Council Bulletin, v. 31, p. 143-146.

Richardson-Bunbury, J.M., 1996, The Kula volcanic field, western Turkey: The development of a Holocene alkali basalt province and the adjacent normal-faulting graben: Geological Magazine, v. 133, p. 275-283.

Rowland, J. V., and Sibson, R. H., 2004, Structural controls on hydrothermal flow in a segmented rift system, Taupo Volcanic Zone, New Zealand: Geofluids, v. 4, p. 259–283.

Rowland, J. V., and Simmons, S. F., 2012, Hydrologic, magmatic, and tectonic controls on hydrothermal flow, Taupo Volcanic Zone, New Zealand: Implications for the formation of epithermal vein deposits: Economic Geology, v. 107, p. 427–457.

Seebeck H, Van Dissen R, Litchfield N, Barnes P, Nicol A, Langridge R, Barrell DJA, Villamor P, Ellis S, Rattenbury M, Bannister S, Gerstenberger M, Ghisetti F, Sutherland R, Fraser J, Nodder S, Stirling M, Humphrey J, Bland K, Howell A, Mountjoy J, Moon V, Stahl T, Spinardi F, Townsend D, Clark K, Hamling I, Cox S, de Lange W, Wopereis P, Johnston M, Morgenstern R, Coffey G, Eccles JD, Little T, Fry B, Griffin J, Townend J, Mortimer N, Alcaraz S, Massiot C, Rowland J, Muirhead J, Upton P, Hirschberg H, Lee J, 2022, New Zealand Community Fault Model – version 1.0. Lower Hutt (NZ): GNS Science. 96 p. (GNS Science report; 2021/57).

Seyitoğlu, G., Tekeli, O., Çemen, I., Şevket, Ş., and Işik, V., 2002, The role of the flexural rotation/rolling hinge model in the tectonic evolution of the Aleşehir graben, western Turkey: Geological Magazine, v. 139, no. 1, p. 15-26.

Shevenell, L., Coolbaugh, M., Hinz, N.H., Stelling, P., Melosh, G., Cumming, W., and Kreemer, C., 2015, Preliminary ranking of geothermal potential in the Cascade and Aleutian volcanic arcs, Part I: Data collection: Geothermal Resources Council Transactions, v. 39, p. 771-784.

Sibson, R.H., and Rowland, JV., 2003, Stress, fluid pressure and structural permeability in seismogenic crust, North Island, New Zealand: Geophysical Journal International, v. 154, p. 584–594, https://doi.org/10.1046/j.1365-246X.2003.01965.x.

Siler, D.L., Hinz, N.H., and Faulds, J.E., 2018, Stress concentrations at structural discontinuities in active fault zones in the western United States: Implications for permeability and fluid flow in geothermal fields: Geological Society of America Bulletin, v. 130, no. 7-8, p. 1273-1288; https://doi.org/10.1130/B31729.1.

Smith, C.M., Faulds, J.E., Brown, S., Coolbaugh, M., DeAngelo, J., Glen, J.M., Burns, E., Siler, D.L., Treitel, S., Mlawsky, E., Fehler, M., Gu, C., and Ayling, B.F., 2023, Exploratory analysis of machine learning techniques in the Nevada geothermal play fairway analysis: Geothermics, v. 111, https://doi.org/10.1016/j.geothermics.2023.102693.

Sözbilir, H., 2001, Extensional tectonics and the geometry of related macroscopic structures: Field evidence from the Gediz detachment, western Turkey: Turkish Journal of Earth Sciences: v. 10, p. 51-67.

Tokçaer, M., Agostini, S., and Savaşçin, M.Y., 2005, Geotectonic setting and origin of the youngest Kula volcanics (western Anatolia), with a new emplacement model: Turkish Journal of Earth Sciences, v. 14, p. 145-166.

Villamor, P., and Berryman, K., 2001, A late Quaternary extension rate in the Taupo Volcanic Zone, New Zealand, derived from fault slip data: New Zealand Journal of Geology and Geophysics, v. 44, p. 243–269. https://doi.org/10.1080/00288306.2001.9514937.

Villamor, P., Berryman, K. R., Nairn, I. A., Wilson, K., Litchfield, N., & Ries, W., 2011, Associations between volcanic eruptions from Okataina volcanic center and surface rupture of nearby active faults, Taupo rift, New Zealand: Insights into the nature of volcano-tectonic interactions: Geological Society of America Bulletin, v. 123, p. 1383-1405.

Villamor, P., Berryman, K.R., Ellis, S.M., Schreurs, G., Wallace, L.M., Leonard, G.S., Langridge, R.M., Ries, W.F., 2017, Rapid evolution of subduction-related continental intra-arc rifts: the Taupo Rift, New Zealand: Tectonics v. 36, p. 2250–2272. https:// doi.org/10.1002/2017TC004715.

Wallace, L.M., Beavan, J., McCaffrey, R., and Darby, D., 2004, Subduction zone coupling and tectonic block rotations in the North Island, New Zealand: Journal of Geophysical Research, v. 109, B12406, doi:10.1029/2004JB003241.

Wallis, I.C., Bardsley, C., Powell, T., Rowland, J.V., and O'Brien, J.M., 2013, A structural model for the Rotokawa geothermal field, New Zealand: Proceedings of the 35th New Zealand Geothermal Workshop, Auckland, New Zealand, Auckland University, p. 17–20.

Wernicke, B., 1992, Cenozoic extensional tectonics of the U.S. Cordillera, *in* Burchfiel, B.C., Lipman, P.W. and Zoback, M.L., eds., The Cordilleran orogen: conterminous U.S.: Boulder, Geological Society of America, The Geology of North America, v. G-3, p. 553-581.

Wilmarth, M., and Stimac, J., 2020, Power Density in Geothermal Fields, 2020 Update: Proceedings World Geothermal Congress, 8 p.

Wigger, N.E., Faulds, J.E., Hampton, S.J., Borella, J.W., and Chambefort, I., 2018, Favorable structural settings for potential geothermal upwellings in the central Taupo volcanic zone, New Zealand: Geological Society of America Abstracts with Programs, v. 50, no. 6, ISSN 0016-7592, doi: 10.1130/abs/2018AM-324134.

Williams, C.F., Reed, M.J., DeAngelo, J., and Galanis, S.P. Jr., 2009, Quantifying the undiscovered geothermal resources of the United States: Geothermal Resources Council Transactions, v. 33, p. 995-1002.

Wilson, C. J. N., and Rowland, J. V., 2016, The volcanic, magmatic and tectonic setting of Taupo Volcanic Zone, New Zealand, reviewed from a geothermal perspective: Geothermics, v. 59, p. 168–187.